Nature of electron trap states under inversion at $In_{0.53}Ga_{0.47}As/Al_2O_3$ interfaces

Davide Colleoni,[1, a] Geoffrey Pourtois,[2] and Alfredo Pasquarello[1]

[1] *Chaire de Simulation à l'Echelle Atomique (CSEA), Ecole Polytechnique Fédérale de Lausanne (EPFL), CH-1015 Lausanne, Switzerland*

[2] *IMEC, Kapeldreef 75, B-3001 Leuven, Belgium*

In and Ga impurities substitutional to Al in the oxide layer resulting from diffusion out of the substrate are identified as candidates for electron traps under inversion at $In_{0.53}Ga_{0.47}As/Al_2O_3$ interfaces. Through density-functional calculations, these defects are found to be thermodynamically stable in amorphous Al_2O_3 and to be able to capture two electrons in a dangling bond upon breaking bonds with neighboring O atoms. Through a band alignment based on hybrid functional calculations, it is inferred that the corresponding defect levels lie at ∼1 eV above the conduction band minimum of $In_{0.53}Ga_{0.47}As$, in agreement with measured defect densities. These results support the technological importance of avoiding cation diffusion into the oxide layer.

The microelectronic industry is investigating high mobility semiconductors for replacing silicon as substrate material. Among the III-V compounds, the $In_xGa_{1-x}As$ family has gathered large interest for application in n-type devices.[1] In particular, the compound $In_{0.53}Ga_{0.47}As$ (here referred to as InGaAs) has suitable electronic properties for microelectronic devices and can easily be grown onto InP substrates.[1,2] Amorphous Al_2O_3 is the preferred dielectric owing to its wide bandgap, high breakdown field, and high thermal stability.[2]

Several passivation procedures have been considered to reduce the high density of interfacial defect states occurring at III-V/oxide interfaces ($D_{\rm it}$).[3–7] The origin of these states has been for long debated and recently assigned to As-As dimer bonds.[8–13] In addition to these interfacial states, a high density of oxide traps ($D_{\rm ot}$) has recently been detected in the oxide layer of metal-oxide-semiconductor (MOS) devices. Capacitance-voltage (CV) measurements show a bimodal distribution for the density of defect states in the oxide,[14] with one peak at 1.5 eV above and the other at 0.5 eV below the CBM of InGaAs. Similarly, through positive bias temperature instability (PBTI) experiments, a wide distribution of defect states centered at about 1 eV above the InGaAs conduction band maximum (CBM) has been inferred.[15] These states are considered to be at the origin of the degradation of the electrical properties, thereby compromising the performance of the corresponding MOS devices.[14,15] Indeed, upon reaching the inversion of carrier population, the Fermi energy is pushed deep into the conduction band of InGaAs in order to achieve high carrier concentrations, and is then susceptible to defects in the upper part of the oxide band gap. The atomic origin of these defects has remained elusive. A hint might come from electrical measurements on $InGaAs/Al_2O_3$ and $Ge/GeO_x/Al_2O_3$ interfaces which yield similar field acceleration factors,[16] but an assessment concerning the nature of the involved defects remains out of reach on this basis. More indicatively, time-of-flight secondary ion mass spectroscopy studies on $GaAs/Al_2O_3$ and $InGaAs/Al_2O_3$ interfaces reveal the presence of In and Ga atoms in the oxide layer due to diffusion from the substrate during oxide deposition.[17,18]

In this work, we investigate isoelectronic In and Ga impurities substitutional to Al in amorphous Al_2O_3 (am-Al_2O_3) in order to evaluate their impact on InGaAs-based devices. We study their thermal stability through density-functional molecular dynamics and determine their electrical properties through the calculation of defect levels. After achieving the band alignment with $In_{0.53}Ga_{0.47}As$ at the hybrid functional level, we find that the calculated defect levels lie in the conduction band of $In_{0.53}Ga_{0.47}As$, making of these impurities good candidates for the observed defect densities.

Structural relaxations and molecular dynamics (MD) are performed with the semilocal functional proposed by Perdew, Burke, and Ernzerhof (PBE).[19] We use a plane-wave basis set determined by a kinetic energy cutoff of 70 Ry together with normconserving pseudopotentials. We sample the Brillouin zone at the sole Γ point, as it has previously been shown that this is sufficient for achieving converged electronic properties.[20] Band gaps and band offsets are evaluated through the hybrid functional proposed by Heyd, Scuseria, and Ernzerhof (HSE).[21] We set the fraction α of Fock exchange to 0.45 in order to reproduce the band gap of crystalline Al_2O_3.[20] The exchange potential is treated as described in Ref. 22. We use the QUANTUM-ESPRESSO suite of programs,[23] with the HSE implementation described in Ref. 24.

We generate isovalent In and Ga defects in am-Al_2O_3 through cyclical structural relaxation in neutral and charged states until structural convergence is achieved.[25] The cycling procedure ensures that defect-independent structural relaxations of the amorphous model do not affect the calculated defect level. We determine defect levels as thermodynamic charge transition levels (ε_{q_1/q_2}).[26–28] When the neutral charge state is involved, a charge transition level is obtained through:

$$\varepsilon_{q_1/0} = \frac{E[X^{q_1}] + E^{q_1}_{\rm corr} - E[X^0]}{q_1} - \epsilon_{\rm v} - \Delta\widetilde{V}, \qquad (1)$$

[a] Electronic mail: davide.colleoni@epfl.ch

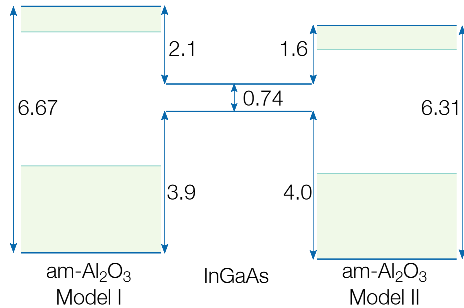

FIG. 1. Band alignment (energies in eV) of models I and II of am-Al_2O_3 with respect to InGaAs, as obtained at the HSE level. Light blue lines indicate the band edges of am-Al_2O_3 as achieved at the PBE level.

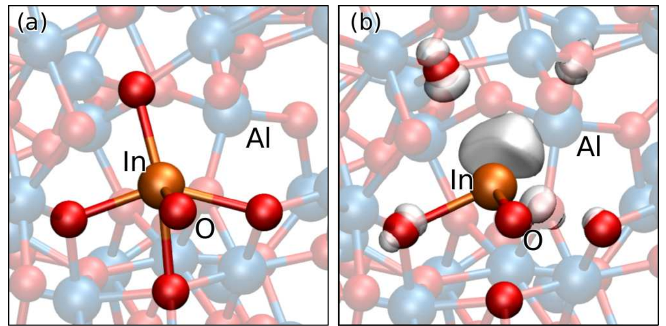

FIG. 2. Defect structure of a representative In_{Al} impurity in am-Al_2O_3, (a) in the neutral and (b) in the charge state $q = -2$. The In atom and its first-neighbor O atoms are highlighted. The isosurface shows the defect charge density.

where $E[X^q]$ is the total energy of the supercell with the cation defect (X) in charge state q and ϵ_v is the valence band maximum (VBM) obtained from a separate bulk calculation. E^q_{corr} is a finite-size correction term obtained through state-of-the-art methods,[27,29] in which we make use of the experimental value of 9.65 as dielectric constant of am-Al_2O_3.[30] For a localized charge with $q = \pm 2$, these corrections amount to 0.7 eV. $\Delta\widetilde{V}$ is a term for aligning the bulk to the charged defect calculations and is achieved through the $2s$ level of twofold coordinated O atoms.[31] In this work, we only focus on charge transition levels, which correspond to relative formation energies. The actual stability of the considered defects is difficult to assess theoretically as absolute defect formation energies depend on elemental chemical potentials, which are poorly characterized during growth.

We consider two models of amorphous Al_2O_3, models I and II, generated previously in Refs. 20 and 32, respectively. Both models contain 160 atoms. Model I has a mass density of 3.31 g/cm^3 and had undergone a treatment to eliminate any residual pressure.[20] For consistency, we imposed the same treatment to model II, which resulted in lattice parameters of $a = 12.2$, $b = 10.5$, and $c = 14.4$ Å. These parameters are slightly larger than the original values in Ref. 32 and lead to a mass density of 2.93 g/cm^3. However, the cell relaxation does not affect the main structural and electronic properties, such as the radial distribution functions, the coordination numbers, and the band gap. We note that the mass density of both models are consistent with the range of experimental values (3.05-3.65 g/cm^3).[33–35]

To refer defect levels calculated in am-Al_2O_3 to the band structure of InGaAs, we need to address the band alignment at the InGaAs/Al_2O_3 interface. We first calculate the band gaps of models I and II at the hybrid functional level finding 6.67 and 6.31 eV, respectively, in accord with measured values, which range from 6.1 to 7.0 eV.[5,36–43] For the line-up with respect to InGaAs, we then use a model of the GaAs/Al_2O_3 interface generated previously[20] and rely on the experimental result that the valence band of InGaAs occurs at essentially the same position as that of GaAs.[43] Using the experimental value of the band gap of InGaAs,[44] we obtain the band alignment shown in Fig. 1. We remark that the present line-up is consistent with a cation terminated substrate, as inferred in previous studies.[20,45] Models I and II of am-Al_2O_3 give almost the same valence band offsets with respect to InGaAs, i.e. 3.9 and 4.0 eV, respectively. The valence band offset calculated here also agrees with a previous theoretical estimate obtained for the interface between InGaAs and the α-phase of Al_2O_3.[46] These results are in line with both experimental and theoretical evidence that the valence bands of different phases of Al_2O_3 line up within a few tenths of electronvolt.[20,47,48] At variance, the different band gaps of the two models lead to significantly different conduction band offsets, i.e. of 2.1 eV and 1.6 eV for models I and II, respectively.

Since the computational cost inherent to the use of a hybrid functional would limit the scope of our investigation, we consider the use of the computationally less expensive PBE functional for the defect-level calculations. Indeed, it has been shown that the energy levels of localized defects achieved with hybrid and semilocal functionals agree closely when referred to the average electrostatic potential.[49–51] The accurate description of the electron density at both the semilocal and hybrid levels underlies the applicability of the present alignment scheme.[52] The use of the PBE functional would therefore preserve the accuracy achieved with hybrid functionals provided the defect levels fall within the PBE band gap. At the PBE level, the band gaps of models I and II of am-Al_2O_3 are 3.6 and 3.4 eV, respectively. The corresponding band alignment is shown in Fig. 1. The PBE band gap of both models of am-Al_2O_3 entirely encloses the band gap of InGaAs. With the PBE functional, we find valence and conduction band offsets of 1.6 and 1.4 eV for model I and of 1.7 and 0.9 eV for model II. This leaves a sufficiently extended energy region around the band gap of InGaAs for the determination of accurate defect levels via the PBE functional.

We consider In and Ga defects substitutional to Al in

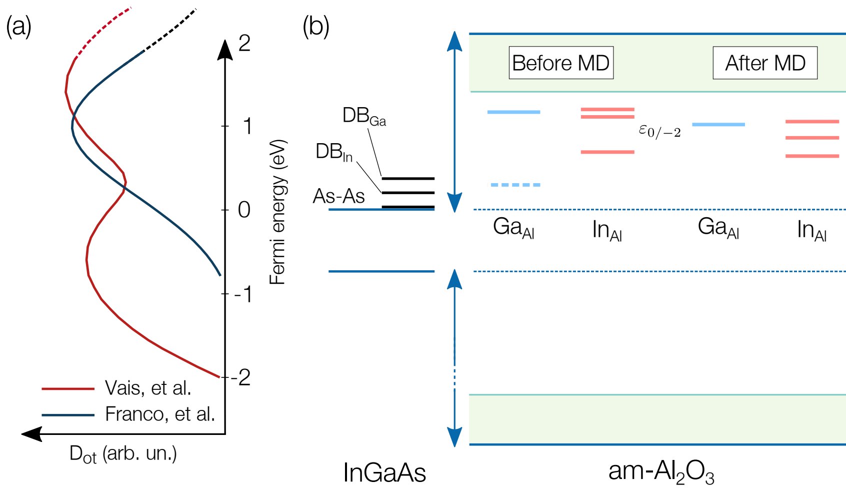

FIG. 3. (a) Experimental density of oxide traps as a function of energy referred to the CBM of InGaAs (from Refs. 15 and 14). (b) Defect levels of In_{Al} and Ga_{Al} defects obtained here, before and after the MD. Only the dashed defect level is associated to a thermodynamical unstable state. We also show calculated energy levels of isolated cations dangling bonds and of the As–As dimer defect (from Ref. 53). The energy scale in panel (a) also applies to the calculated defect levels in panel (b).

our models of am-Al_2O_3. Both In and Ga impurities are investigated in ten Al sites differing by their nearest neighbor environment, which may contain either four or five O atoms. Since In, Ga, and Al are all trivalent atoms, In_{Al} and Ga_{Al} defects are electronically isovalent to the pristine defect-free model. We thus expect the formation of an electronically active defect to be associated to the breaking of cation-O bonds and thus to the formation of either empty or doubly occupied dangling bonds. Besides the neutral state, we therefore investigate In_{Al} and Ga_{Al} defects in doubly positive and doubly negative charge states.

Among the twenty different defects considered in this work, we find three In_{Al} and two Ga_{Al} defects with localized defect states. In the following, we focus on these defects and discard the electrically inactive ones. In the neutral charge state, neither In_{Al} nor Ga_{Al} defects induce significant structural rearrangement around the defect. For In_{Al} defects, we only observe a slight outward relaxation of the first coordination-shell to accomodate the size of the In cation. In all cases, the resulting local environment remains the same as that of the substituted Al atom in the pristine model.

For the retained defects, the defect level always involves the charge state -2. The charge state $+2$ does not yield any stable state. In a few cases, we also checked the charge state -1 and found it to be unstable. In the -2 charge state, large structural rearrangements occur upon the capture of two extra electrons. We generally observe the breaking of a few cation-O bonds and the formation of a doubly-occupied dangling bond on the cation impurity, as shown for a representative In impurity in Fig. 2. The first-neighbor shell of the defect then typically only counts either two or three O atoms (cf. Supplemental Material). The associated defect levels lie in the upper part of the am-Al_2O_3 band gap, corresponding to the conduction band of the InGaAs [cf. Fig. 3(b)]. We remark that the important relaxation is critical to stabilize the charge state -2 and thus to produce a defect level in the investigated energy region.

To assess their thermodynamical stability during the oxide deposition, we perform MD simulations for $\sim$3 ps at 1000 K. This procedure is effective in removing energy levels of unstable defects from the band gap.[25,54] Since the Fermi energy lies within the semiconductor band gap during the oxide deposition, the MD is performed with the defects in their neutral charge state [cf. Fig. 3(b)]. We find that the neutral defect structures undergo on average a stabilization of $\sim$0.7 eV, which can be assigned to increased first-neighbor coordinations of either five or six O atoms upon MD. The thermally equilibrated defect structures are then further relaxed in the -2 and neutral charge states through relaxation cycles.[25] Upon the addition of two electrons, we observe the same structural rearrangements described for the defects before MD, leading to undercoordinated cation impurities with only two or three bonded O atoms. The defect levels calculated after the MD treatment generally fall in the upper part of the am-Al_2O_3 band gap covering an energy region which closely corresponds to that obtained before MD [Fig. 3(b)]. Only in one case, the MD treatment reveals a thermodynamically unstable state and leads to the disappearence of its defect level [dashed in Fig. 3(b)]. Thus, our annealing procedure generally validates the picture achieved prior to the MD.

The calculated defect levels largely depend on the structural rearrangements that can be achieved to stabilize the charge state -2 and are therefore sensitive to the varying structural environment in the amorphous. Indeed, they show a large spread and extend from 5.2 to 5.8 eV above the VBM of am-Al_2O_3. Hence, at InGaAs/Al_2O_3 interfaces, these defect levels fall deep into the conduction band of InGaAs, between 0.7 and 1.3 eV above the CBM. The defect levels of In_{Al} and Ga_{Al} closely correspond to the peak in the measured density of oxide traps[14,15] occurring at about 1 eV above the CBM of InGaAs [Fig. 3(a)]. The nature of these oxide defects should be considered distinct compared to those contributing to the experimental density of interface states, which does not extend above the CBM of InGaAs by more than a few tenths of an electronvolt.[5–7,55] Similarly, their extension within the conduction band of

InGaAs is significantly more pronounced than found in previous studies[53] on interfacial defects [cf. black lines on the left in Fig. 3(b)]. The present results indicate that In and Ga impurities, which have diffused from the substrate into the oxide, produce unoccupied defect levels in flat-band conditions when the Fermi energy lies below the CBM of InGaAs. However, when a sufficiently high stress potential is applied as upon inversion, these states can act as electron traps.

In conclusion, we identified In and Ga atoms incorporated in the amorphous oxide layer of Al_2O_3 as origin of the electron traps observed upon inversion at $In_{0.53}Ga_{0.47}As/Al_2O_3$ interfaces. In_{Al} and Ga_{Al} defects can capture two electrons in doubly occupied dangling bonds upon breaking bonds with first-neighbor O atoms. The calculated defect levels agree with the defect density measured in PBTI and CV experiments. Since these defects are expected to affect the performance of corresponding MOS devices, special care should be devoted to avoiding their out-diffusion from the substrate.

Financial support is acknowledged from the Swiss National Science Foundation (Grants No. 200020-152799). DC thanks M. Heyns and G. Pourtois for supporting a one-month site visit at IMEC. We used computational resources of CSCS and CSEA-EPFL.

[1] J. A. del Alamo, Nature **479**, 317 (2011).
[2] S. Oktyabrsky and P. D. Ye, eds., *Fundamentals of III-V Semiconductor MOSFETs* (Springer, 2009).
[3] D. Lin, A. Alian, S. Gupta, B. Yang, E. Bury, S. Sioncke, R. Degraeve, M. L. Toledano, R. Krom, P. Favia, H. Bender, M. Caymax, K. C. Saraswat, N. Collaert, and A. Thean, in *IEDM* (2012) p. 28.3.1.
[4] L. K. Chu, C. Merckling, A. Alian, J. Dekoster, J. Kwo, M. Hong, M. Caymax, and M. Heyns, Appl. Phys. Lett. **99**, 042908 (2011).
[5] I. Krylov, B. Pokroy, M. Eizenberg, and D. Ritter, J. Appl. Phys. **120**, 124505 (2016).
[6] G. Brammertz, H. Lin, K. Martens, A.-R. Alian, C. Merckling, J. Penaud, D. Kohen, W.-E. Wang, S. Sioncke, A. Delabie, M. Meuris, M. R. Caymax, and M. Heyns, ECS Trans. **19**, 375 (2009).
[7] Y. C. Chang, W. H. Chang, C. Merckling, J. Kwo, and M. Hong, Appl. Phys. Lett. **102**, 093506 (2013).
[8] L. Lin and J. Robertson, Applied Physics Letters **98**, 082903 (2011).
[9] G. Miceli and A. Pasquarello, Appl. Phys. Lett. **103**, 041602 (2013).
[10] A. Stesmans, S. Nguyen, and V. V. Afanas'ev, Appl. Phys. Lett. **103**, 162111 (2013).
[11] D. Colleoni, G. Miceli, and A. Pasquarello, J. Phys.: Condens. Matter **26**, 492202 (2014).
[12] D. Colleoni, G. Miceli, and A. Pasquarello, Phys. Rev. B **92**, 125304 (2015).
[13] J. Robertson, Y. Guo, and L. Lin, J. Appl. Phys. **117**, 112806 (2015).
[14] A. Vais, J. Franco, H.-C. Lin, N. Collaert, A. Mocuta, K. De Meyer, and A. Thean, Appl. Phys. Lett. **107**, 223504 (2015).
[15] J. Franco, A. Alian, B. Kaczer, D. Lin, T. Ivanov, A. Pourghaderi, K. Martens, Y. Mols, D. Zhou, N. Waldron, S. Sioncke, T. Kauerauf, N. Collaert, A. Thean, M. Heyns, and G. Groeseneken, in *IEEE International Reliability Physics Symposium (IRPS)* (2014) p. 6A.2.1.
[16] G. Groeseneken, J. Franco, M. Cho, B. Kaczer, M. Toledano-Luque, P. Roussel, T. Kauerauf, A. Alian, J. Mitard, H. Arimura, D. Lin, N. Waldron, S. Sioncke, L. Witters, H. Mertens, L.-A. Ragnarsson, M. Heyns, N. Collaert, A. Thean, and A. Steegen, in *IEEE International Electron Devices Meeting (IEDM)* (2014) p. 34.4.1.
[17] M. Caymax, G. Brammertz, A. Delabie, S. Sioncke, D. Lin, M. Scarrozza, G. Pourtois, W.-E. Wang, M. Meuris, and M. Heyns, Microelectron. Eng. **86**, 1529 (2009).
[18] A. Alian, G. Brammertz, R. Degraeve, M. Cho, C. Merckling, D. Lin, W. E. Wang, M. Caymax, M. Meuris, K. D. Meyer, and M. Heyns, IEEE Electron Device Lett. **33**, 1544 (2012).
[19] J. P. Perdew, K. Burke, and M. Ernzerhof, Phys. Rev. Lett. **77**, 3865 (1996).
[20] D. Colleoni, G. Miceli, and A. Pasquarello, Appl. Phys. Lett. **107**, 211601 (2015).
[21] J. Heyd, G. E. Scuseria, and M. Ernzerhof, J. Chem. Phys. **118**, 8207 (2003); **124**, 219906 (2006).
[22] P. Broqvist, A. Alkauskas, and A. Pasquarello, Phys. Rev. B **80**, 085114 (2009).
[23] P. Giannozzi, S. Baroni, N. Bonini, M. Calandra, R. Car, C. Cavazzoni, D. Ceresoli, G. L. Chiarotti, M. Cococcioni, I. Dabo, A. Dal Corso, S. de Gironcoli, S. Fabris, G. Fratesi, R. Gebauer, U. Gerstmann, C. Gougoussis, A. Kokalj, M. Lazzeri, L. Martin-Samos, N. Marzari, F. Mauri, R. Mazzarello, S. Paolini, A. Pasquarello, L. Paulatto, C. Sbraccia, S. Scandolo, G. Sclauzero, A. P. Seitsonen, A. Smogunov, P. Umari, and R. M. Wentzcovitch, J. Phys: Condens. Matter **21**, 395502 (2009).
[24] H.-P. Komsa, P. Broqvist, and A. Pasquarello, Phys. Rev. B **81**, 205118 (2010).
[25] P. Broqvist and A. Pasquarello, Microelectron. Eng. **84**, 2022 (2007).
[26] C. G. Van de Walle and J. Neugebauer, J. Appl. Phys. **95**, 3851 (2004).
[27] H.-P. Komsa, T. T. Rantala, and A. Pasquarello, Phys. Rev. B **86**, 045112 (2012).
[28] C. Freysoldt, B. Grabowski, T. Hickel, J. Neugebauer, G. Kresse, A. Janotti, and C. G. Van de Walle, Rev. Mod. Phys. **86**, 253 (2014).
[29] C. Freysoldt, J. Neugebauer, and C. G. Van de Walle, Phys. Rev. Lett. **102**, 016402 (2009).
[30] H. Momida, T. Hamada, Y. Takagi, T. Yamamoto, T. Uda, and T. Ohno, Phys. Rev. B **73**, 054108 (2006).
[31] H.-P. Komsa and A. Pasquarello, Phys. Rev. B **84**, 075207 (2011).
[32] K. Sankaran, L. Goux, S. Clima, M. Mees, J. A. Kittl, M. Jurczak, L. Altimime, G.-M. Rignanese, and G. Pourtois, ECS Trans. **45**, 317 (2012).
[33] P. Lamparter and R. Kniep, Physica B **234236**, 405 (1997).
[34] Y. Oka, T. Takahashi, K. Okada, and S.-I. Iwai, J. Non-Cryst. Solids **30**, 349 (1979).
[35] S.-M. Lee, D. G. Cahill, and T. H. Allen, Phys. Rev. B **52**, 253 (1995).
[36] S. Miyazaki, J. Vac. Sci. Technol. B **19**, 2212 (2001).
[37] H. Y. Yu, M. F. Li, B. J. Cho, C. C. Yeo, M. S. Joo, D.-L. Kwong, J. S. Pan, C. H. Ang, J. Z. Zheng, and S. Ramanathan, Appl. Phys. Lett. **81**, 376 (2002).
[38] K. Y. Gao, T. Seyller, L. Ley, F. Ciobanu, G. Pensl, A. Tadich, J. D. Riley, and R. G. C. Leckey, Appl. Phys. Lett. **83**, 1830 (2003).
[39] M. L. Huang, Y. C. Chang, C. H. Chang, T. D. Lin, J. Kwo, T. B. Wu, and M. Hong, Appl. Phys. Lett. **89**, 012903 (2006).
[40] J. Ahn, I. Geppert, M. Gunji, M. Holland, I. Thayne, M. Eizenberg, and P. C. McIntyre, Appl. Phys. Let. **99**, 232902 (2011).
[41] I. Krylov, D. Ritter, and M. Eizenberg, J. Appl. Phys. **117**, 174501 (2015).
[42] N. V. Nguyen, O. A. Kirillov, W. Jiang, W. Wang, J. S. Suehle, P. D. Ye, Y. Xuan, N. Goel, K.-W. Choi, W. Tsai, and S. Sayan, Appl. Phys. Let. **93**, 082105 (2008).
[43] V. V. Afanasev, A. Stesmans, G. Brammertz, A. Delabie, S. Sionke, A. O'Mahony, I. M. Povey, M. E. Pemble, E. OConnor, P. K. Hurley, and S. B. Newcomb, Appl. Phys. Lett. **94**,

202110 (2009).
[44]G. Brammertz, H.-C. Lin, M. Caymax, M. Meuris, M. Heyns, and M. Passlack, Appl. Phys. Lett. **95**, 202109 (2009).
[45]G. Miceli and A. Pasquarello, Appl. Phys. Lett. **102**, 201607 (2013).
[46]M. Choi, A. Janotti, and C. G. Van de Walle, J. Appl. Phys. **113**, 044501 (2013).
[47]S. Toyoda, T. Shinohara, H. Kumigashira, M. Oshima, and Y. Kato, Appl. Phys. Lett. **101**, 231607 (2012).
[48]E. O. Filatova and A. S. Konashuk, J. Phys. Chem. C **119**, 20755 (2015).
[49]A. Alkauskas, P. Broqvist, and A. Pasquarello, Phys. Rev. Lett. **101**, 046405 (2008).
[50]J. L. Lyons, A. Janotti, and C. G. Van de Walle, Phys. Rev. B **80**, 205113 (2009).
[51]H. Peng, D. O. Scanlon, V. Stevanovic, J. Vidal, G. W. Watson, and S. Lany, Phys. Rev. B **88**, 115201 (2013).
[52]A. Alkauskas, P. Broqvist, and A. Pasquarello, Phys. Status Solidi B **248**, 775 (2011).
[53]D. Colleoni, G. Miceli, and A. Pasquarello, Microelectron. Eng. **147**, 260 (2015).
[54]Z. Guo, F. Ambrosio, and A. Pasquarello, Appl. Phys. Lett. **109**, 062903 (2016).
[55]G. Brammertz, H.-C. Lin, K. Martens, D. Mercier, S. Sioncke, A. Delabie, W. E. Wang, M. Caymax, M. Meuris, and M. Heyns, Appl. Phys. Lett. **93**, 183504 (2008).